Electronic Supplementary Material (ESI) for ChemComm.

Supporting Information

Synthesis and resolution of multi-chiral carbonyl-N embedded hetero[7]helicenes for efficient circularly polarized luminescence

Yuxiang Wang,* Qi Liao, Yabin Feng, Yiran Wang, Yunzhi Li,* Qi Meng*

School of Petrochemical Engineering, Changzhou University, Jiangsu Key Laboratory of Advanced Catalytic Materials and Technology, Changzhou, Jiangsu 213164, P. R. China; Email: wangyx@cczu.edu.cn; mengqi@cczu.edu.cn

School of Chemistry and Chemical Engineering, Linyi University, Linyi, Shandong 276000, P. R. China; Email: liyunzhi@lyu.edu.cn

Table of Contents

1. Measurements

Nuclear magnetic resonance (NMR) spectra were recorded on 300 or 400 MHz Bruker spectrometer. Ultraviolet-visible (UV-*vis*) spectra were recorded on Shimadzu UV-1700 UV-*vis* spectrophotometer. Emission spectra were performed on Agilent Cary Eclipse spectrophotometer. The transient photoluminescence (PL) decay spectra and absolute PL quantum yield were determined by Edinburgh FS5 Fluorescence Spectrometer. Circular dichroism (CD) spectra were measured from a JASCO J-810 spectropolarimeter. CPL spectra were measured from a JASCO CPL-300 spectrofluoropolarimeter. Thermogravimetric analysis (TGA) was performed by using a Netzsch TG 209 F3 Tarsus under N_2 atmosphere. Cyclic voltammetry (CV) was measured on a CHI920C (Shanghai CH Instrument Company, China) electrochemical workstation in CH_2Cl_2 solution at room temperature under N_2 atmosphere, with $TBAPF_6$ (0.1 M) as supporting electrolyte and a Hg/Hg_2Cl_2 electrode as a reference electrode. The enantiomeric excesses were confirmed by chiral HPLC using an Agilent Technologies 1260 Infinity with a CHIRALPAK® ZWIX(-)(ZM30LI-CO012) column.

2. Synthesis procedures of the chiral hetero[7]helicenes

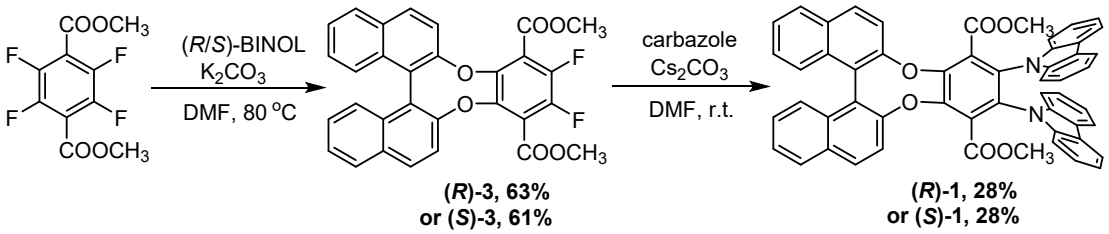

Scheme S1. The Synthesis procedures of **(*R*/*S*)-1**.

Synthesis of (*R*/*S*)-3:

A mixture of (*S*)-BINOL (500.0 mg, 1.75 mmol) and anhydrous potassium carbonate (2.41 g, 10.48 mmol) in dry DMF (10 mL) was stirred for 2 h at room temperature. After addition of a solution of dimethyl 2,3,5,6-tetrafluoroterephthalate (511.2 mg, 1.92 mmol) in dry DMF (5mL), the mixture was stirred for 12 h under N_2 atmosphere at 80 ℃. After cooling to room temperature, the reaction mixture was quench with water and extracted with ethyl acetate. The organic phase was dried with anhydrous Na_2SO_4 and the solvent was evaporated. The reaction mixture was purified by column chromatography (petroleum ether/ethyl acetate = 10:1) to afford **(*S*)-3** (543.0 mg, 61 %) as white powder. **(*R*)-3** (554.0 mg, 63 %) was synthesized in the same procedure from (*R*)-BINOL.

(*S*)-3: ^{1}H NMR (300 MHz, $CDCl_3$): δ 8.02 (d, J = 8.9 Hz, 2H), 7.96 (d, J = 8.3 Hz, 2H), 7.71 (d, J

=8.9 Hz, 2H), 7.53-7.48 (m, 2H), 7.22 (td, J_1= 6.9 Hz, J_2= 1.2 Hz 1H), 3.98 (s, 3H). ^{13}C NMR (400 MHz, $CDCl_3$): δ 162.20, 150.22, 145.5, 142.67, 142.07, 132.14, 132.04, 131.27, 128.59, 127.10, 126.79, 126.01, 125.51, 120.92, 53.53. HRMS (ESI, m/z): caled for $C_{30}H_{19}F_2O_6$ [M+H$^+$], 531.1144; found, 513.1150. caled for $C_{30}H_{18}F_2O_6Na$ [M+Na$^+$], 535.0964; found, 535.0969.

Synthesis of (*R*/*S*)-1:

A mixture of carbazole (0.75 g, 4.51 mmol) and Cs_2CO_3 (1.75 g，5.37 mmol) in dry DMF (20 mL) was stirred for 2 h at room temperature. After the addition of a solution of **(*S*)-3** (1.10 g, 2.15 mmol) in dry DMF (15 mL), the mixture was stirred for 12 h under N_2 atmosphere at room temperature. After terminated with aqueous ammonium chloride, the reaction mixture was extracted with ethyl acetate and washed with water. The organic phase was dried with anhydrous Na_2SO_4 and the solvent was evaporated. The reaction mixture was purified by column chromatography (petroleum ether/dichloroethane = 15:1) to afford **(*S*)-1** (480.0 mg, 28 %) as white powder. **(*R*)-1** (483 mg, 28 %) was synthesized in the same procedure from **(*R*)-3**.

(*S*)-1: ^{1}H NMR (400 MHz, $CDCl_3$): δ 8.15 (d, J = 8.8 Hz, 1H), 8.03 (d, J = 7.9 Hz, 2H), 7.95 (d, J = 8.8 Hz, 2H), 7.70 (d, J = 7.7 Hz, 2H), 7.66-7.63 (m, 1H), 7.55 (t, J = 7.5 Hz, 2H), 7.40(td, J_1 = 8.0 Hz ,J_2 = 1.0 Hz, 2H), 7.27 (q, J = 8.1 Hz, 2H), 7.09 (td, J_1= 7.4Hz, J_2= 1.0 Hz ,1H), 7.05-7.03 (m ,1H) , 6.97-6.91 (m, 2H), 3.17(s, 3H). ^{13}C NMR (400 MHz, $CDCl_3$): δ 163.98, 150.30, 147.08, 140.67, 140.55, 132.30, 132.18, 132.10, 131.38, 128.63, 127.13, 126.91, 126.09, 125.59, 125.33, 125.13, 123.69, 123.33, 121.31, 120.33, 120.12, 119.81, 119.55, 52.74. HRMS (ESI, m/z): caled for $C_{54}H_{35}N_2O_6^+$ [M+H$^+$], 807.2490; found, 807.2493; caled for $C_{54}H_{34}N_2NaO_6^+$ [M+Na$^+$], 829.2309; found, 829.2308.

Synthesis of DCzAO1 and **DCzAO2** from **(*R*/*S*)-1:**

(*S*)-1 (500.0 mg, 7.8 mmol) was dissolved in 10 mL ethylene glycol and 5 mL 1.55 M aqueous KOH. The mixture was heated at 120 ℃ for 24 h. After cooling to room temperature, the reaction mixture was acidified to pH = 2-3 by dilute hydrochloric acid. The precipitated white solid was collected by vacuum filtration, washed thoroughly with water and ethanol, dried under vacuum to afford hydrolysis product (452.0 mg, 99%) which can be used in the next step without further purification.

The hydrolysis product of **(*S*)-1** (100.0 mg, 128.4 μmol) was dispersed in 5 mL anhydrous dichloromethane with the addition of thionyl chloride (93 μL, 1.28 mmol) and two drops of

anhydrous DMF. After 3 h under reflux, anhydrous aluminium chloride (102.7 mg, 770.4 μmol) was added. After refluxing for 12 h, the reaction mixture was cooled to room temperature, and quenched by adding water dropwise under vigorous stirring. The resulting mixture was diluted with dichloromethane, washed with water and then dried over anhydrous Na_2SO_4. The solvent was evaporated under reduced pressure and the yellow solid product was purified by column chromatography on silica gel (petroleum ether: ethyl acetate = 10:1) to yield the mixture of **(*S,P*)-DCzAO1** and **(*S,M*)-DCzAO2** as orange solid (42.1 mg, 42 %). **(*S,P*)-DCzAO1** and **(*S,M*)-DCzAO2** can be identified qualitatively by thin-layer chromatography (petroleum ether: toluene =1:10, Figure S1) and quantitatively by ^{1}H NMR spectrum (Figure S26). The mixture of **(*R,M*)-DCzAO1** and **(*R,P*)-DCzAO2** were synthesized from **(*R*)-1** by the same procedures.

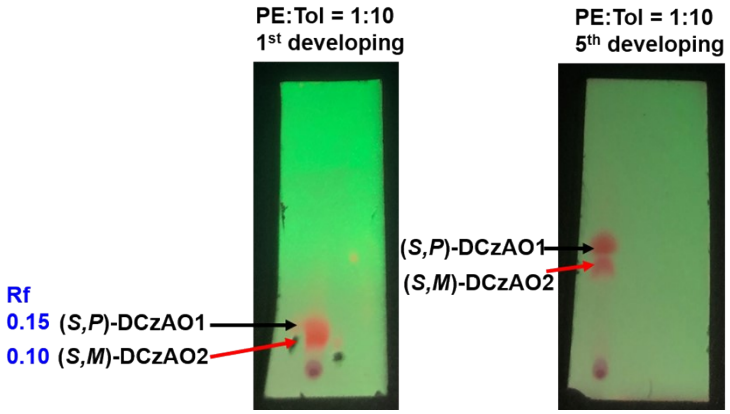

Figure S1. TLC analysis of the mixture of **(*S,P*)-DCzAO1** and **(*S,M*)-DCzAO2**.

Synthesis of DCzAO1 and **DCzAO2** from **(*R*/*S*)-2:**

(*R*/*S*)-2 was synthesized according to literature reported procedure (*J. Am. Chem. Soc.*, 2016, **138**, 3990-3993). To a solution of **(*R*/*S*)-2** (600.0 mg, 0.81 mmol) in 50 mL 1,2-dichloroethane was added triflic acid (1.94 mL, 24.3 mmol). The reaction mixture was stirred at room temperature for 12 h and monitored by TLC. After the full consumption of **(*R*/*S*)-2**, 25 mL water and 25 mL dioxane were added to the reaction mixture. After hydrolyzed at 80°C for 12 h, the reaction mixture was extracted with dichloromethane and washed with water. The organic phase was separated, dried over anhydrous Na_2SO_4 and evaporated under reduced pressure. The residual was purified by column chromatography on silica gel (petroleum ether: ethyl acetate = 10:1) to yield the mixture of **(*R,M*)-DCzAO1** and **(*R,P*)-DCzAO2** (394.0 mg, 65 %) or the mixture of **(*S,P*)-DCzAO1** and **(*S,M*)-DCzAO2** (382.0 mg, 64 %) as orange solid.

Separation of DCzAO1 and **DCzAO2:**

The mixture of **(*S*,*P*)-DCzAO1** and **(*S*,*M*)-DCzAO2** (350 mg) was dissolved in 40 mL ethyl acetate under reflux. **(*S*,*P*)-DCzAO1** (104.5 mg) was obtained after cooling, crystallization and filtration. The residual solution was evaporated and the second part of **(*S*,*P*)-DCzAO1** 103.0 mg) could be recrystallized from 15 mL ethyl acetate. The totally separated amount of **(*S*,*P*)-DCzAO1** was 207.5 mg with 89 % recovery. Then 1,2-dichloroethane and n-hexane (3 mL, 1/1, v/v) were used in the recrystallization of the residual to yield **(*S*,*M*)-DCzAO2** as orange solid (69.0 mg, 59 % recovery). **(*R*,*M*)-DczAO1** (207.6 mg, 90 % recovery) and **(*R*,*P*)-DczAO2** (70.5 mg, 61 % recovery) were separated by the similar procedure from the mixture of **(*R*,*M*)-DczAO1 and (*R*,*P*)-DczAO2** (346.7 mg).

(*S*,*P*)-DCzAO1: ^{1}H NMR (400 MHz, $CDCl_3$): δ 8.47 (dd, J_1 = 7.8 Hz, J_2 = 0.6 Hz, 1H), 8.33 (d, J = 7.4 Hz, 1H), 8.02 (d, J = 8.8 Hz, 1H), 7.95 (t, J = 8.8 Hz, 2H), 7.86 (d, J = 7.6 Hz, 1H), 7.71(t, J_1 = 7.0 Hz , 2H), 7.50 (t, J = 7.4 Hz, 2H), 7.41 (t, J= 7.7 Hz, 2H), 7.01 (t, J = 7.32 Hz, 1H), 6.71 (t, J = 7.9 Hz, 1H), 6.23(d, J = 8.4 Hz , 1H). ^{13}C NMR (75 MHz, C_6D_6): δ 176.73, 152.06, 146.60, 138.95, 137.17, 132.69, 132.40, 131.21, 128.83, 127.59, 126.39, 126.70, 126.49, 125.27, 124.71, 123.55, 123.36, 122.10, 121.23, 121.02, 120.79, 112.07. HRMS (ESI, m/z): caled for $C_{52}H_{27}N_2O_4$ [M+H$^+$], 743.1965; found, 743.19695; caled for $C_{52}H_{26}N_2NaO_4$ [M+Na$^+$], 765.1785; found, 765.17800.

(*S*,*M*)-DCzAO2: ^{1}H NMR (400 MHz, $CDCl_3$): δ 8.54 (dd, J_1 = 7.8 Hz, J_2 = 0.8 Hz, 1H), 8.38 (dd, J = 7.46 Hz, J_2 = 0.8 Hz, 1H), 7.91 (t, J = 8.96 Hz, 3H), 7.77 (t, J = 7.7 Hz, 1H), 7.71 (d, J = 8.84 Hz, 2H), 7.48(td, J_1 = 6.9 Hz , J_2 = 1.2 Hz, 1H), 7.40 (td, J_1 = 7.7 Hz, J_2 =1.3 Hz, 1H), 7.02 (t, J= 7.96 Hz, 1H), 6.71 (t, J = 7.9 Hz, 1H), 6.23 (d, J = 8.4 Hz, 1H). ^{13}C NMR (75 MHz, $CDCl_3$): δ 177.28, 151.05, 147.18, 139.33, 137.68, 132.33, 131.99, 130.66, 128.38, 127.27, 126.92, 126.56, 126.18, 126.09, 125.97, 125.45, 124.77, 124.52, 123.24, 122.95, 121.36, 121.10, 112.09. HRMS (ESI, m/z): caled for $C_{52}H_{27}N_2O_4$ [M+H$^+$], 743.1965; found, 743.19633; caled for $C_{52}H_{26}N_2NaO_4$ [M+Na$^+$], 765.1785; found, 765.17819.

3. Chiral HPLC analysis of the chiral hetero[7]helicenes

The enantiomeric excesses (*ee*) were confirmed by chiral HPLC using an Agilent 1260 Infinity instrument with a Daicel CHIRALPAK® ZWIX(-)(ZM30LI-CO012) column. Mobile phase: MeOH/ACN = 75/25 (v/v) + (50 mM Formic acid + 25 mM Diethylamine), sample solution: 0.1 mg/mL in THF/Water = 80/20 (v/v), solvent flow rate: 0.4 mL/min, detector wavelength: 254 nm.

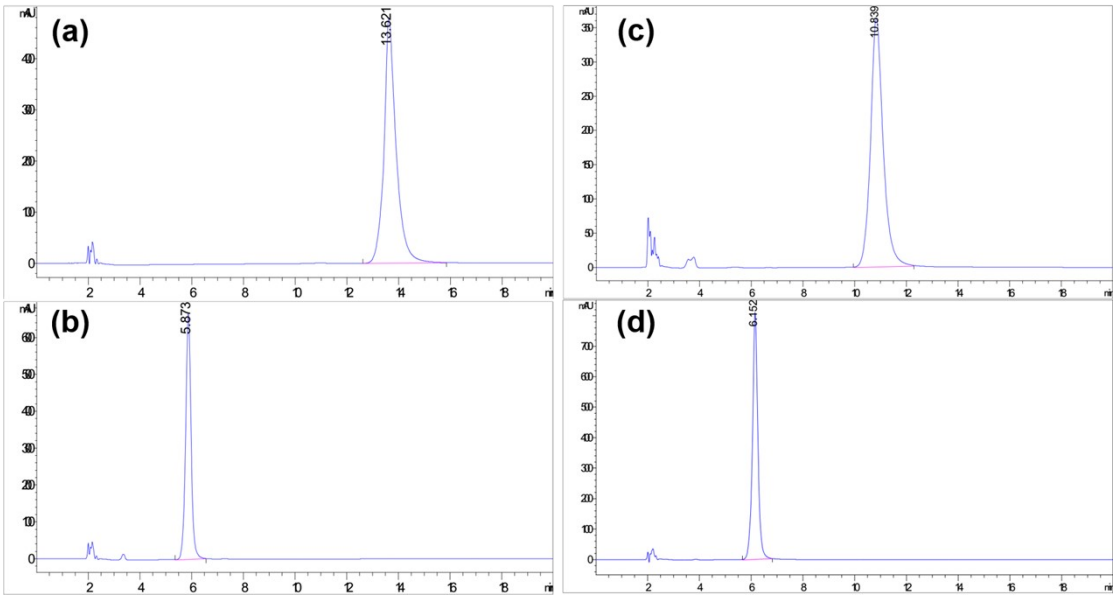

Figure S2. Chiral HPLC spectra of (a) (***R***,***M***)**-DCzAO1**, (b) (***S***,***P***)**-DCzAO1**, (c) (***R***,***P***)**-DCzAO2** and (d) (***S***,***M***)**-DCzAO2**.

Table S1. Chiral HPLC data of the chiral hetero[7]helicenes.

Compound	Ret. Time (min)	Area (a.u.)	Area (%)	*ee* (%)
(***R***,***M***)**-DCzAO1**	13.621	15619.630	100	100
(***S***,***P***)**-DCzAO1**	5.873	9801.824	100	100
(***R***,***P***)**-DCzAO2**	10.839	12369.865	100	100
(***S***,***M***)**-DCzAO2**	6.152	11723.072	100	100

4. TGA curves of the chiral hetero[7]helicenes

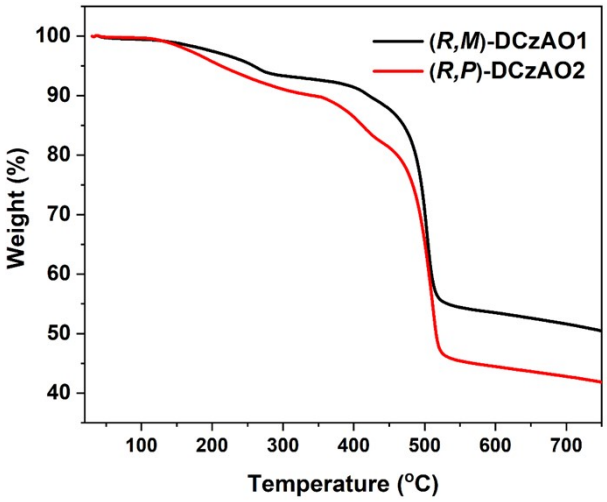

Figure S3. The TGA curves of (***R,M***)**-DCzAO1** and (***R,P***)**-DCzAO2.**

5. Crystal data of the chiral hetero[7]helicenes

The single crystals of (***R,M***)**-DCzAO1** and (***R,P***)**-DCzAO2** were obtained by volatilizing the solution in CH_2Cl_2/Hexane at room temperature. X-ray data at 100 K were examined on a Bruker SMART APEX II Single-Crystal X-Ray Diffractometer using MoKα radiation (λ = 0.71073 Å). The structures were solved by direct methods and refined with the full-matrix least square technique. The details of crystal data and structure refinement were presented in Table S2. The crystal data of (***R,M***)**-DCzAO1** and (***R,P***)**-DCzAO2** were deposited to CCDC with CCDC number of 2314296 and 2314297.

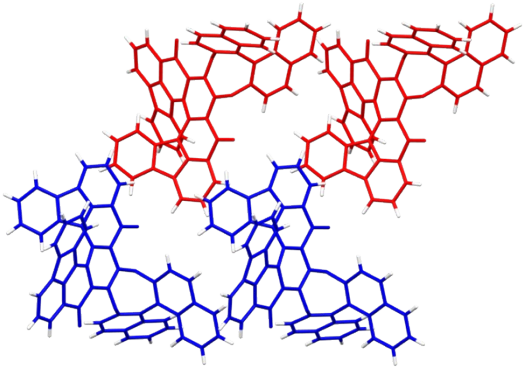

Figure S4. Molecular packing of (***R,M***)**-DCzAO1** in the single crystal, the molecules in the alternating parallel layers with different orientations were colored in different colors.

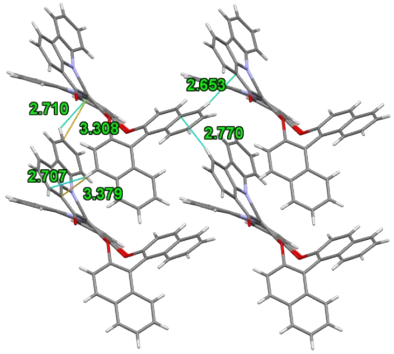

Figure S5. Intermolecular C-H···π (blue line) and C···C (orange line) interactions in the stacking structures of (***R,M***)**-DCzAO1**.

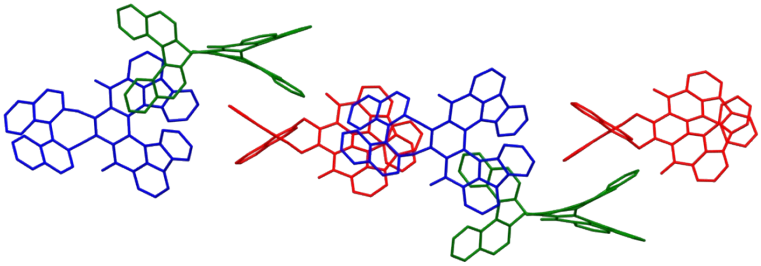

Figure S6. Molecular packing of (***R,P***)**-DCzAO2** in the single crystal, the molecules in the alternating parallel layers with different orientations were colored in different colors.

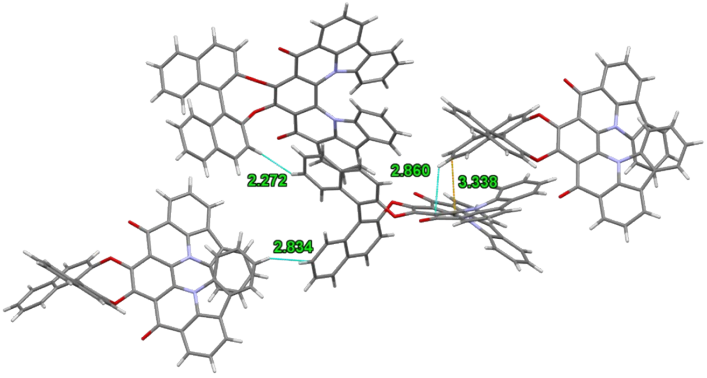

Figure S7. Intermolecular C-H···π (blue line) and C···C (orange line) interactions in the stacking structures of (***R,P***)**-DCzAO2**.

Table S2. Crystal data and structure refinement for the chiral hetero[7]helicenes.

Compound	(*R*,*M*)-DCzAO1	(*R*,*P*)-DCzAO2
CCDC	2314296	2314297
Empirical formula	$C_{52}H_{26}N_2O_4$	$C_{52}H_{26}N_2O_4$
Formula weight	742.7893	742.7893
Temperature/K	100	100
Crystal system	monoclinic	hexagonal
Space group	$P2_1$	$P6_1$
a/Å	8.1505(5)	13.1642(13)
b/Å	11.3911(8)	13.1642(13)
c/Å	20.8223(13)	48.250(6)
α/°	90	90
β/°	92.329(2)	90
γ/°	90	120
Volume/Å^3	1931.6(2)	7241.3(17)
Z	2	6
ρ_{calc} g/cm^3	1.423	1.259
μ/mm^{-1}	0.223	0.078
F(000)	852.0	2904.0
Crystal size/mm^3	0.12 × 0.04 × 0.02	0.12 × 0.08 × 0.04
Radiation	MoKα (λ = 0.71073)	MoKα (λ = 0.71073)
2Θ range for data collection/°	3.916 to 52.83	4.38 to 52.736
Index ranges	-10 ≤ h ≤ 10, -12 ≤ k ≤ 14, -26 ≤ l ≤ 26	-16 ≤ h ≤ 15, -11 ≤ k ≤ 16, -52 ≤ l ≤ 57
Reflections collected	14940	33338
Independent reflections	6770 [R_{int} = 0.0753, R_{sigma} = 0.1027]	9239 [R_{int} = 0.1303, R_{sigma} = 0.1497]
Data/restraints/parameters	6770/1/550	9239/888/681
Goodness-of-fit on F^2	1.051	0.991
Final R indexes [I>=2σ (I)]	R_1 = 0.0589, wR_2 = 0.1223	R_1 = 0.0754, wR_2 = 0.1612
Final R indexes [all data]	R_1 =0.0922, wR_2 =0.1453	R_1 = 0.1582, wR_2 = 0.2032
Largest diff. peak/hole / e Å^{-3}	0.44/-0.31	0.39/-0.32
Flack parameter	0.08(8)	-0.8(10)

6. Electrochemical properties of the chiral hetero[7]helicenes

Table S3. Electrochemical properties of the chiral hetero[7]helicenes

	E_{OX} [V]	$^{a}E_{HOMO}$ [eV]	$^{b}E_{g,opt}$ [eV]	$^{c}E_{LUMO}$ [eV]
(***R,M***)**-DCzAO1**	0.60	-5.07	2.34	-2.73
(***R,P***)**-DCzAO2**	0.48	-4.95	2.30	-2.65

$^{a}E_{HOMO}$ = -[E_{OX} - $E_{(Fc/Fc+)}$ + 4.8] eV; $^{b}E_{g,opt}$ = 1240/λ_{onset}; $^{c}E_{LUMO}$ = $E_{g,opt}$ + E_{HOMO}.

7. Photophysical Properties of the chiral hetero[7]helicenes

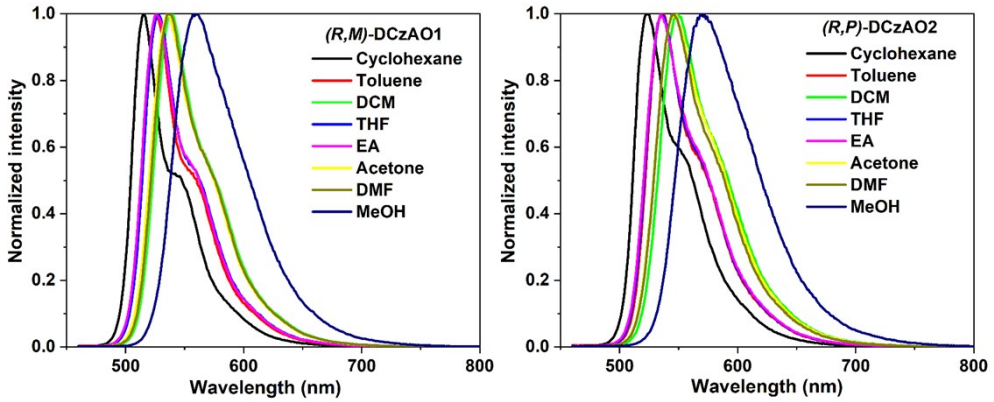

Figure S8. Solvatochromic PL spectra of (***R,M***)**-DCzAO1** and (***R,P***)**-DCzAO2** (λ_{ex} = 450 nm, 1 × 10^{-5} M).

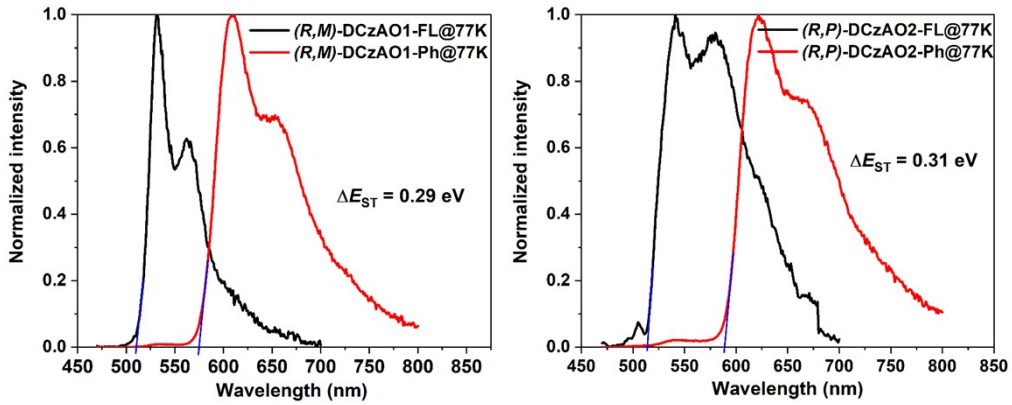

Figure S9. Fluorescence and phosphorescence spectra of (***R,M***)**-DCzAO1** and (***R,P***)**-DCzAO2** in toluene solutions at 77 K (1 × 10^{-5} M).

The preparation procedure of the doped films: The doped films in this work were prepared by drop-casting. To be specific, 5 mg of chiral hetero[7]helicene and 95 mg of PMMA (purchased from Energy Chemical Co., average Mw 20 kDa) were dissolved in 5 mL of toluene. The obtained solution (50 μL) was drop-casted onto the quartz plate (1 mm × 10 mm × 40 mm). After annealing at 80 ℃ for 2 h, the resulting doped films were subjected to the following tests.

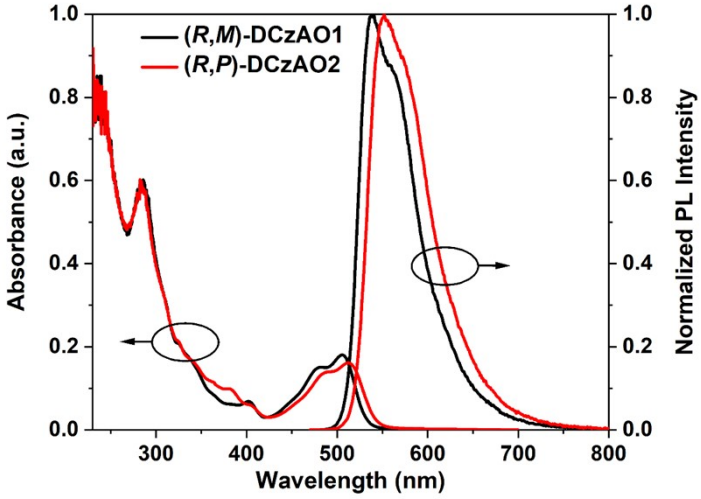

Figure S10. Absorption and PL spectra of **(*R*,*M*)-DCzAO1** and **(*R*,*P*)-DCzAO2** in doped films (5 wt% in PMMA).

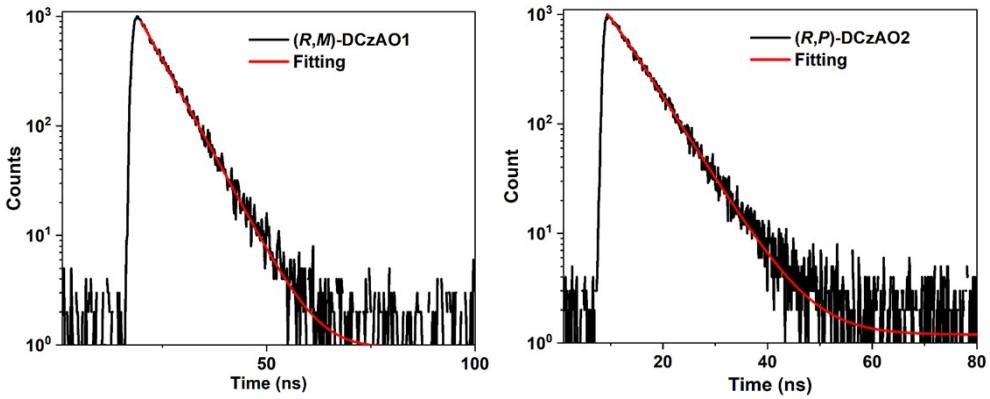

Figure S11. Transient PL spectra of **(*R*,*M*)-DCzAO1** and **(*R*,*P*)-DCzAO2** in toluene solutions (1 × 10^{-5} M).

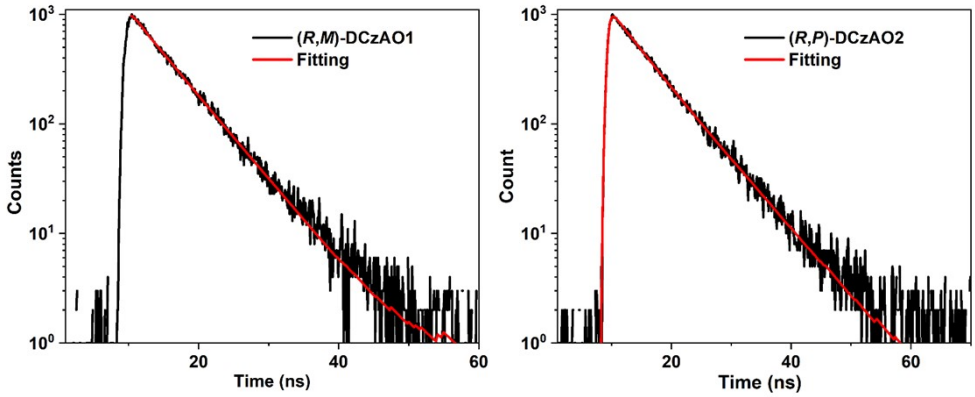

Figure S12. Transient PL spectra of **(*R*,*M*)-DCzAO1** and **(*R*,*P*)-DCzAO2** in doped films (5 wt% in PMMA).

Table S4. The photophysical data of **(*R*,*M*)-DCzAO1** and **(*R*,*P*)-DCzAO2**.

compound	λ_{abs} (nm)	λ_{em} (nm)	Φ_{PL} (%)	τ (ns)	FWHM (nm)	ΔE_{ST} (eV)
(*R*,*M*)-DCzAO1[a]	402,479, 506	525	57	6.2	47	0.29
(*R*,*M*)-DCzAO1[b]	284, 404, 480, 505	538	50	5.9	68	
(*R*,*P*)-DCzAO2[a]	404,487, 513	535	55	5.5	53	0.31
(*R*,*P*)-DCzAO2[b]	283, 382, 486, 513	553	47	7.3	73	

[a]In toluene solutions (1×10^{-5} M). [b]In doped films (5 wt% in PMMA).

8. Chiroptical properties of the chiral hetero[7]helicenes

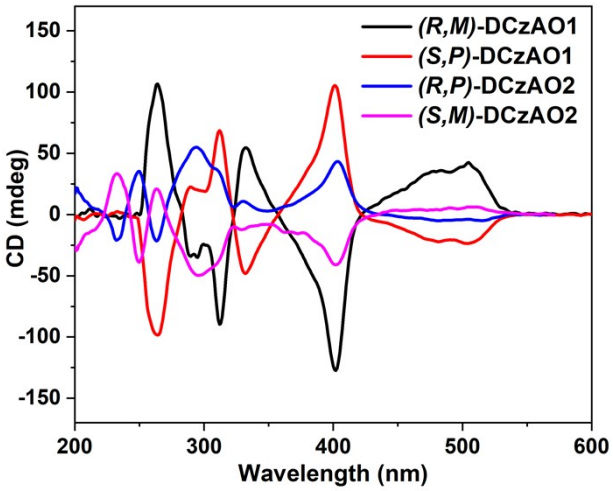

Figure S13. CD spectra of the chiral hetero[7]helicenes in doped films (5 wt% in PMMA).

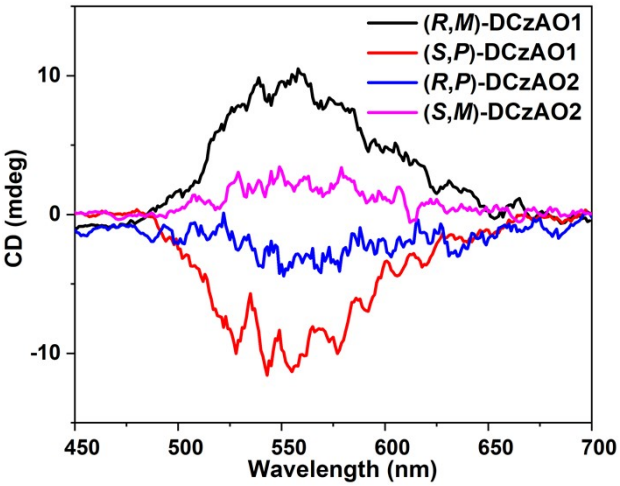

Figure S14. CPL spectra of the chiral hetero[7]helicenes in doped films (5 wt% in PMMA).

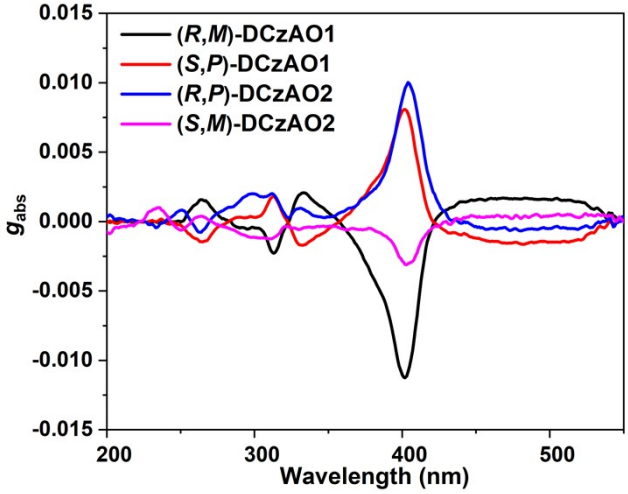

Figure S15. Curves of g_{abs} values versus wavelength for the chiral hetero[7]helicenes in doped films (5 wt% in PMMA).

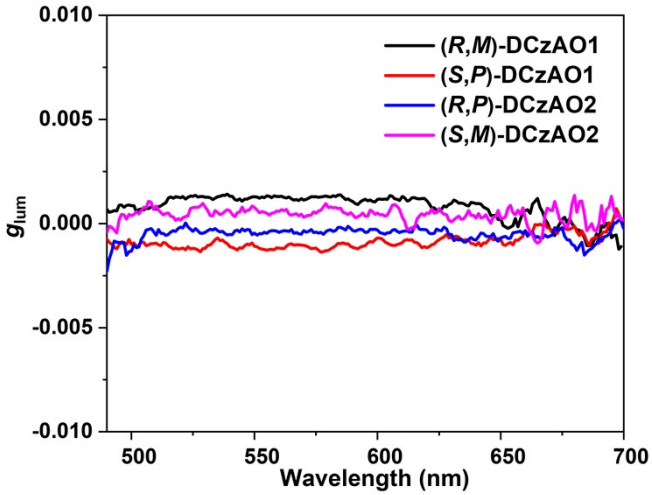

Figure S16. Curves of g_{lum} values versus wavelength for the chiral hetero[7]helicenes in doped films (5 wt% in PMMA).

Table S5. The chiroptical parameters of the chiral hetero[7]helicenes.

Compound	toluene solution				doped film			
	λ_{CD} (nm)	g_{abs} (10^{-3})	λ_{CPL} (nm)	g_{lum} (10^{-3})	λ_{CD} (nm)	g_{abs} (10^{-3})	λ_{CPL} (nm)	g_{lum} (10^{-3})
***(R,M)*-DCzAO1**	504	2.0	550	1.4	513	1.5	527	1.3
***(S,P)*-DCzAO1**		-1.9		-1.3		-1.5		-1.3
***(R,P)*-DCzAO2**	516	-0.70	555	-0.5	512	-0.5	553	-0.5
***(S,M)*-DCzAO2**		0.70		0.8		0.5		0.6

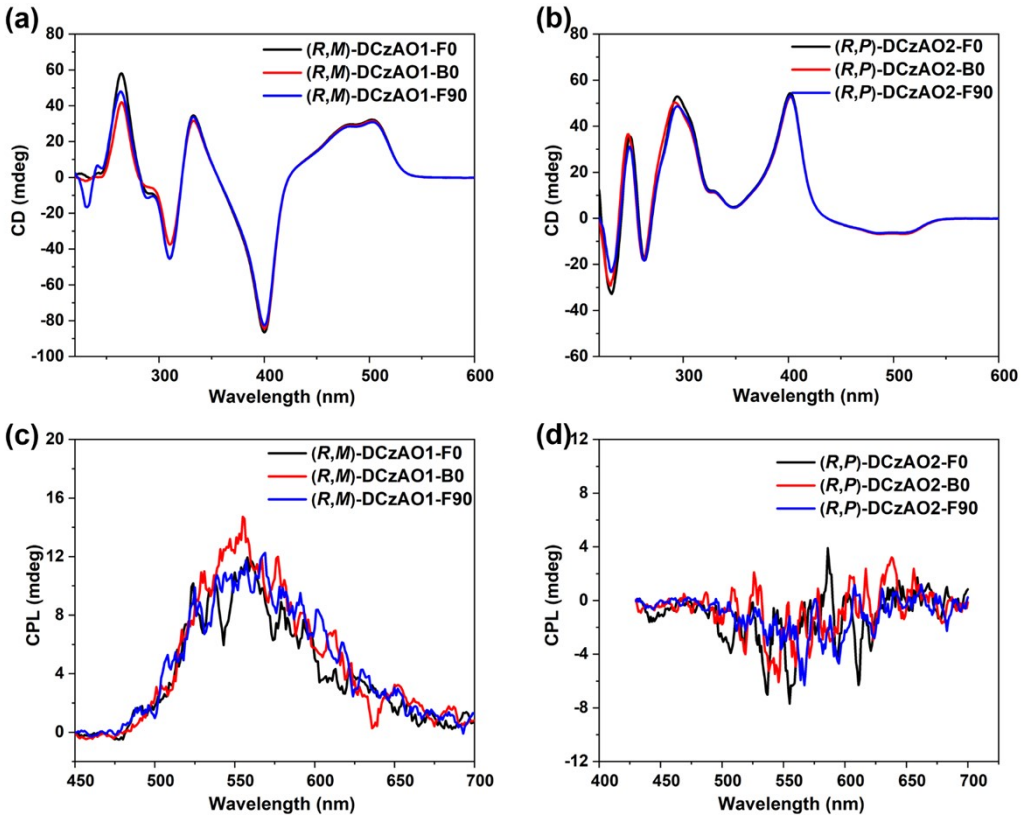

Figure S17. The CD and CPL spectra of the chiral hetero[7]helicenes in doped films (5 wt% in PMMA) from different sides and rotation angles, F0: front side 0º rotation, B0: back side 0º rotation, F90: front side 90º rotation.

9. NMR and HRMS Spectra of all new compounds

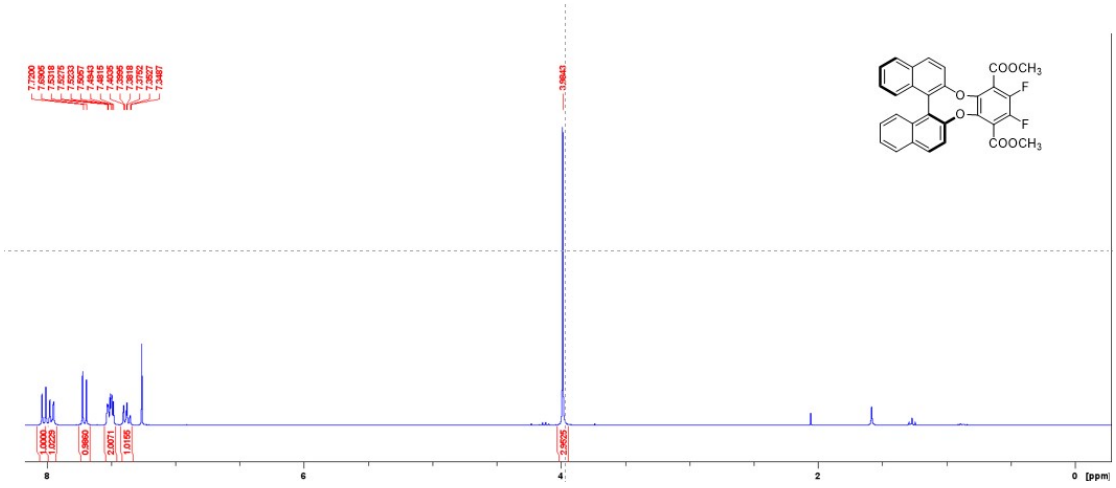

Figure S18. ^{1}H NMR spectrum of ***S*-2** (400 MHz, $CDCl_3$).

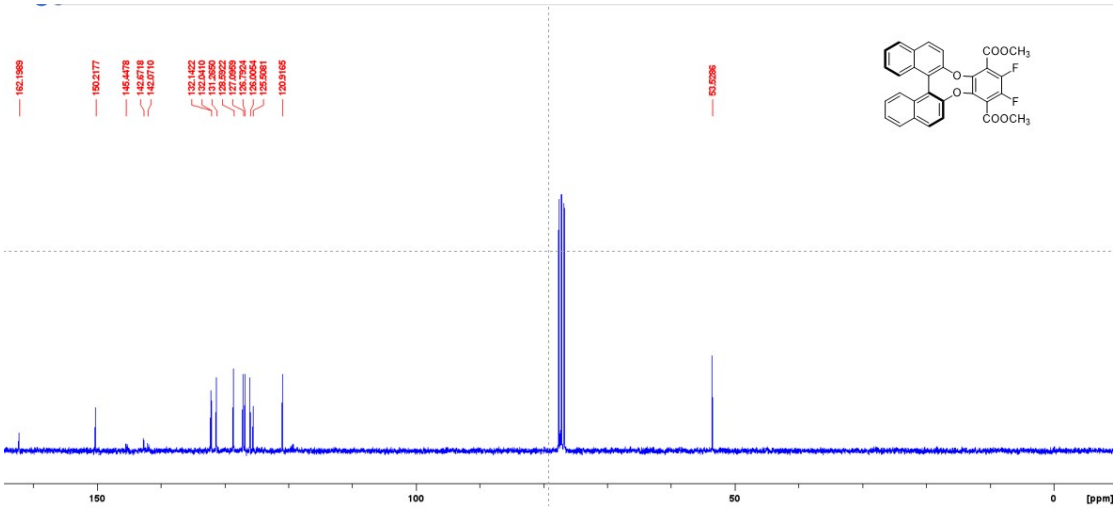

Figure S19. ^{13}C NMR spectrum of ***S*-2** (75 MHz, $CDCl_3$)

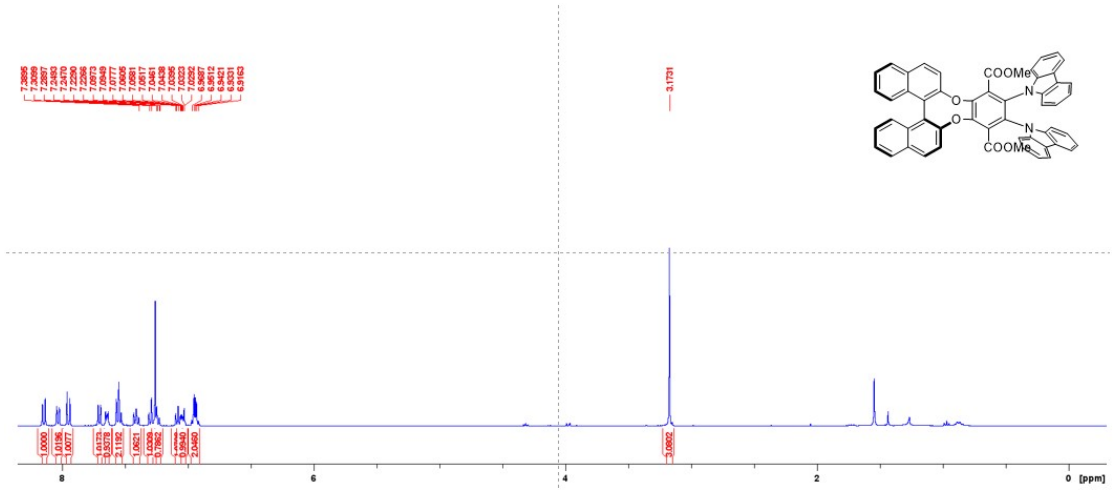

Figure S20. ^{1}H NMR spectrum of ***S*-3** (400 MHz, $CDCl_3$).

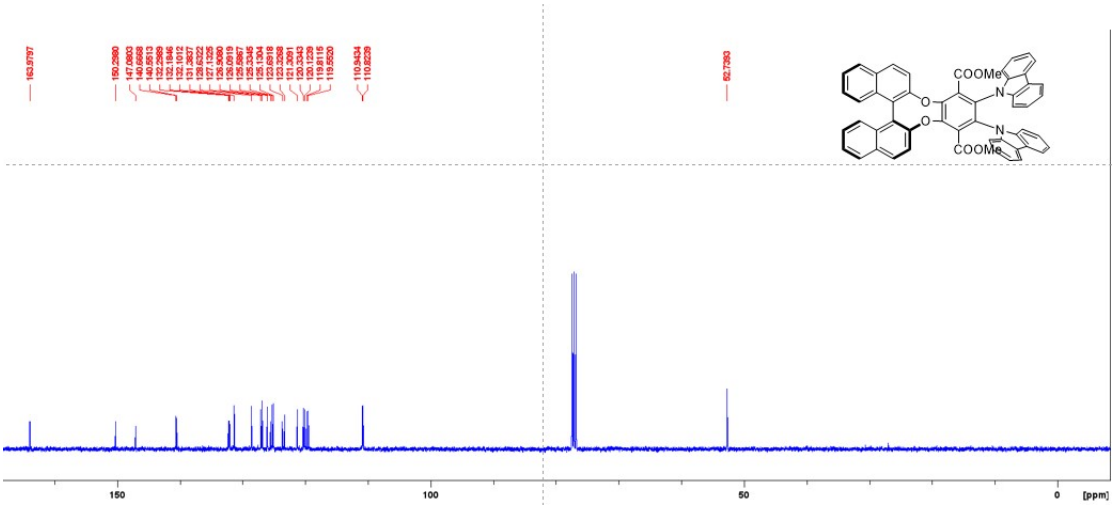

Figure S21. ^{13}C NMR spectrum of ***S*-3** (75 MHz, $CDCl_3$)

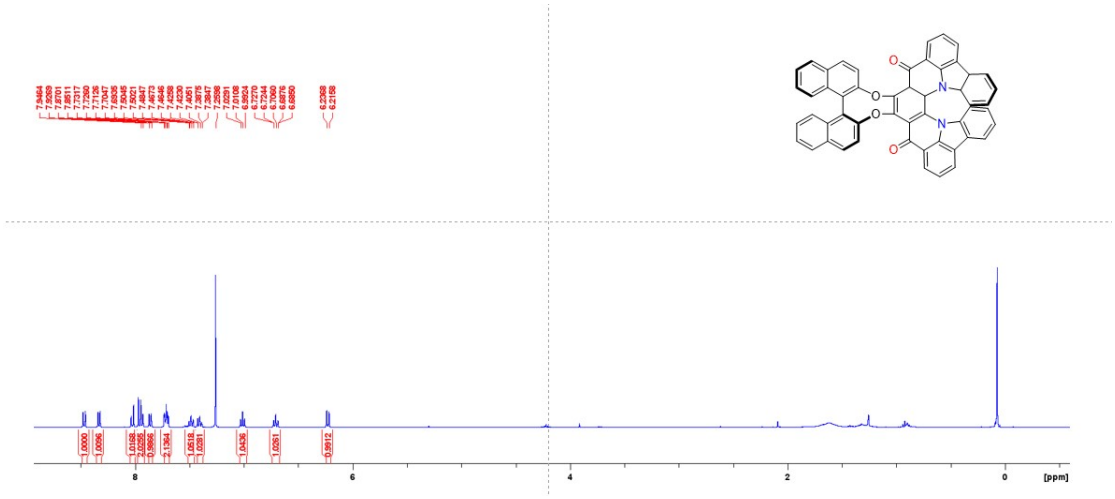

Figure S22. ^{1}H NMR spectrum of **(*S*,*P*)-DCzAO1** (400 MHz, $CDCl_3$).

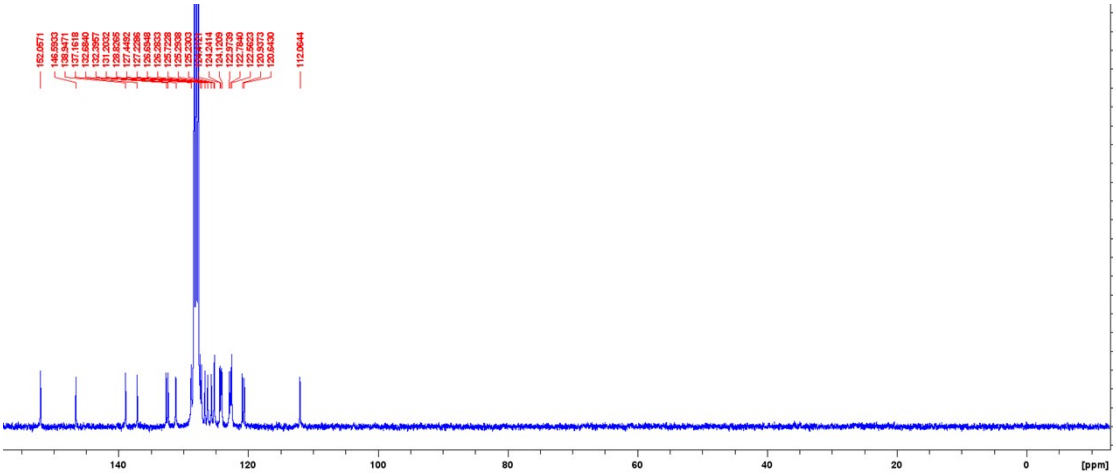

Figure S23. ^{13}C NMR spectrum of **(*S*,*P*)-DCzAO1** (75 MHz, C_6D_6).

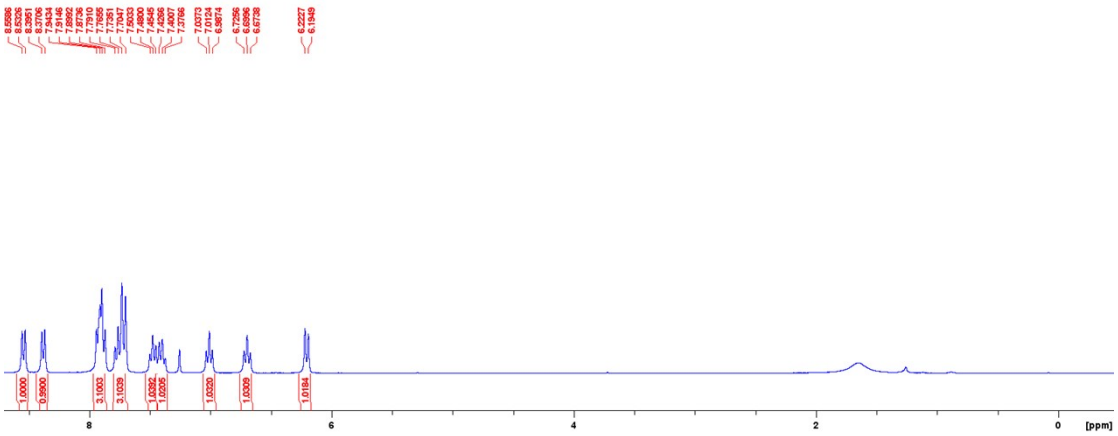

Figure S24. ^{1}H NMR spectrum of **(*S*,*M*)-DCzAO2** (300 MHz, $CDCl_3$).

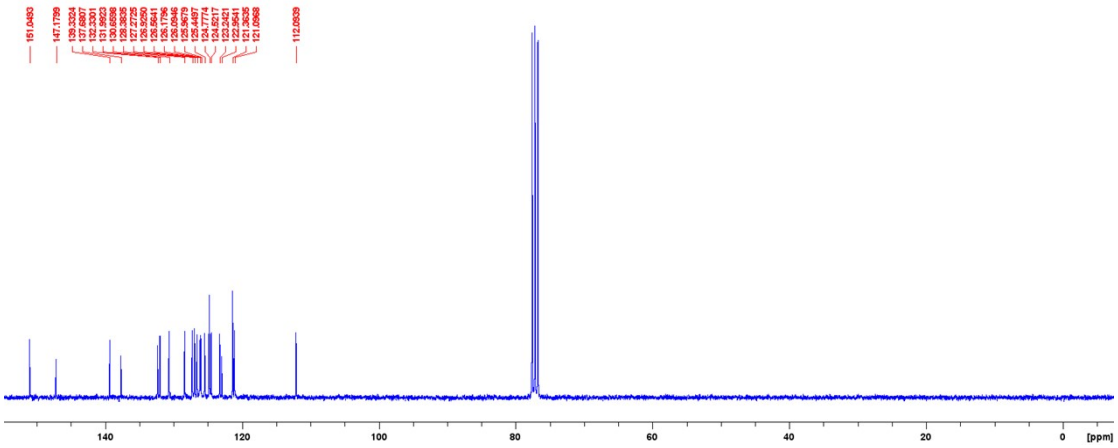

Figure S25. ^{13}C NMR spectrum of **(*S*,*M*)-DCzAO2** (75 MHz, $CDCl_3$).

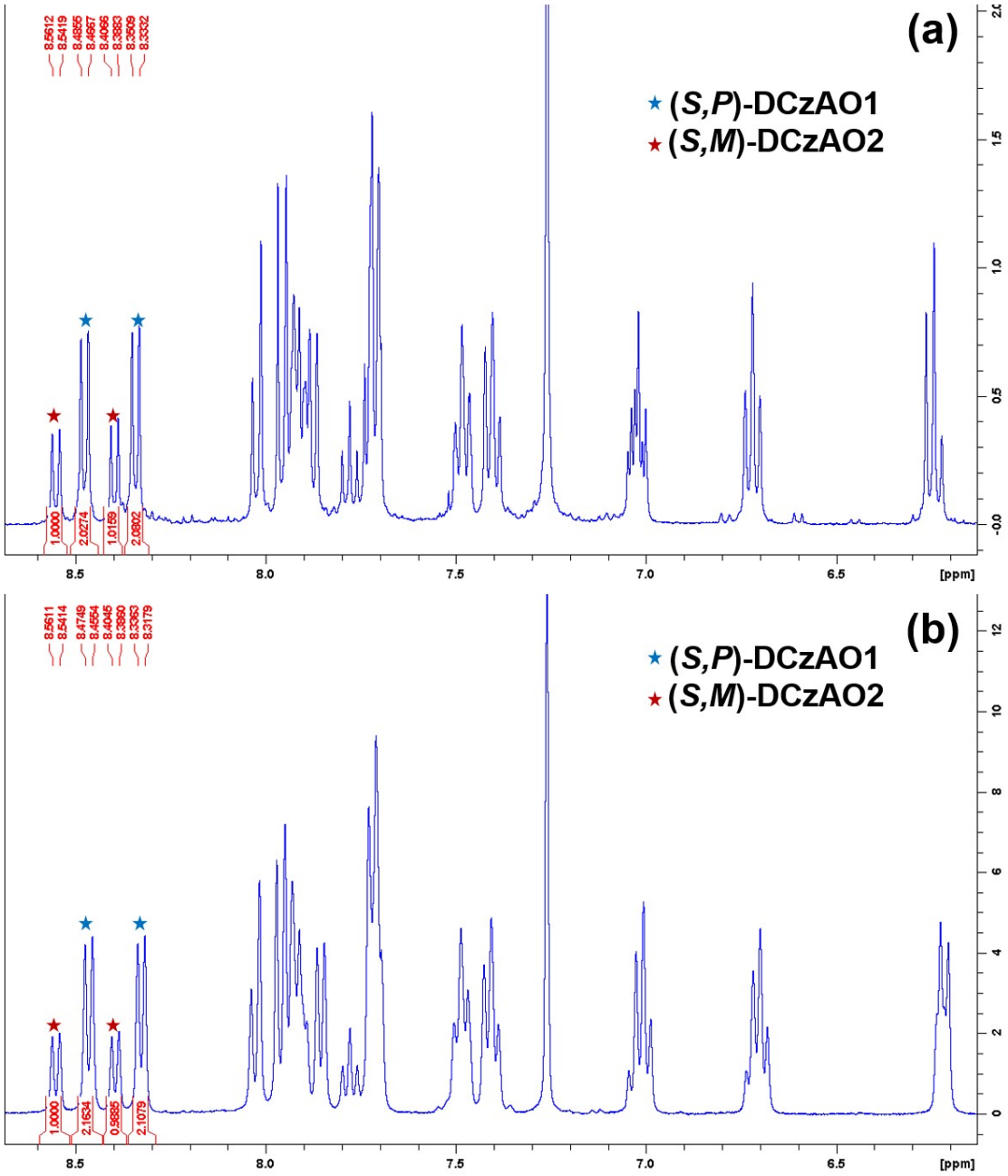

Figure S26. ^{1}H NMR spectrum (400 MHz, $CDCl_3$) for the mixture of **(*S*,*P*)-DCzAO1** and **(*S*,*M*)-DCzAO2** acquired from (a) route A and (b) route B.

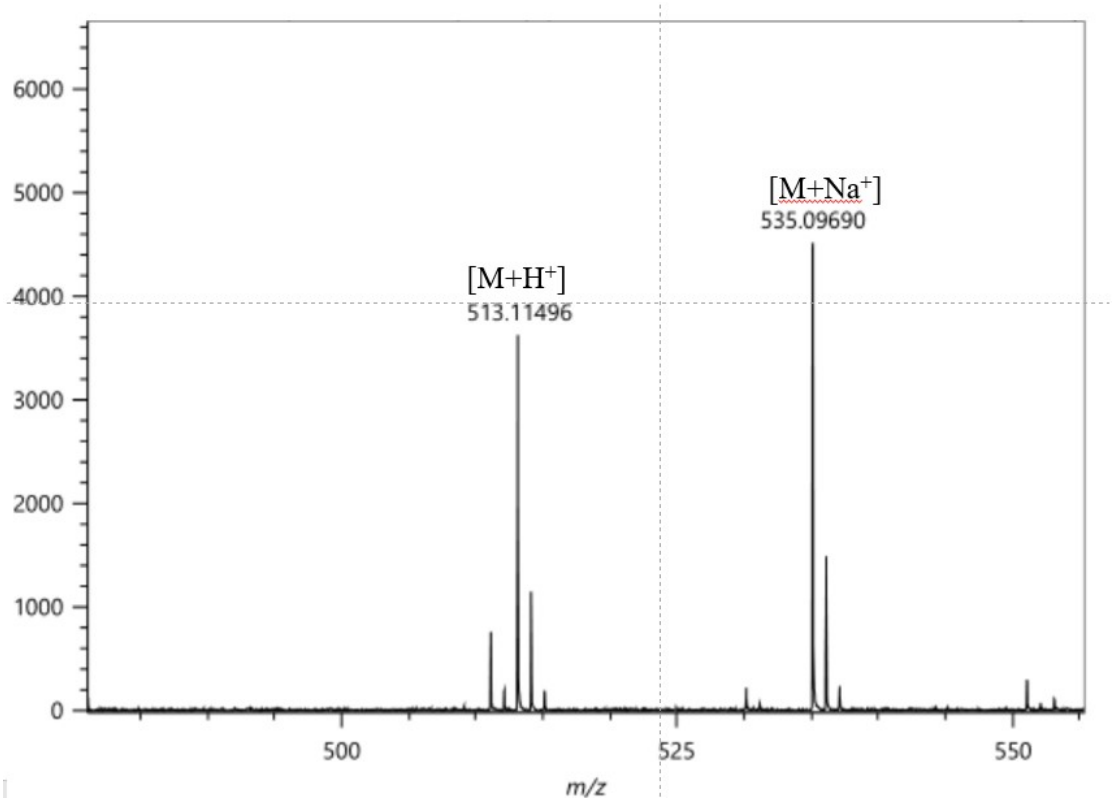

Figure S27. HRMS spectra of ***S*-2**.

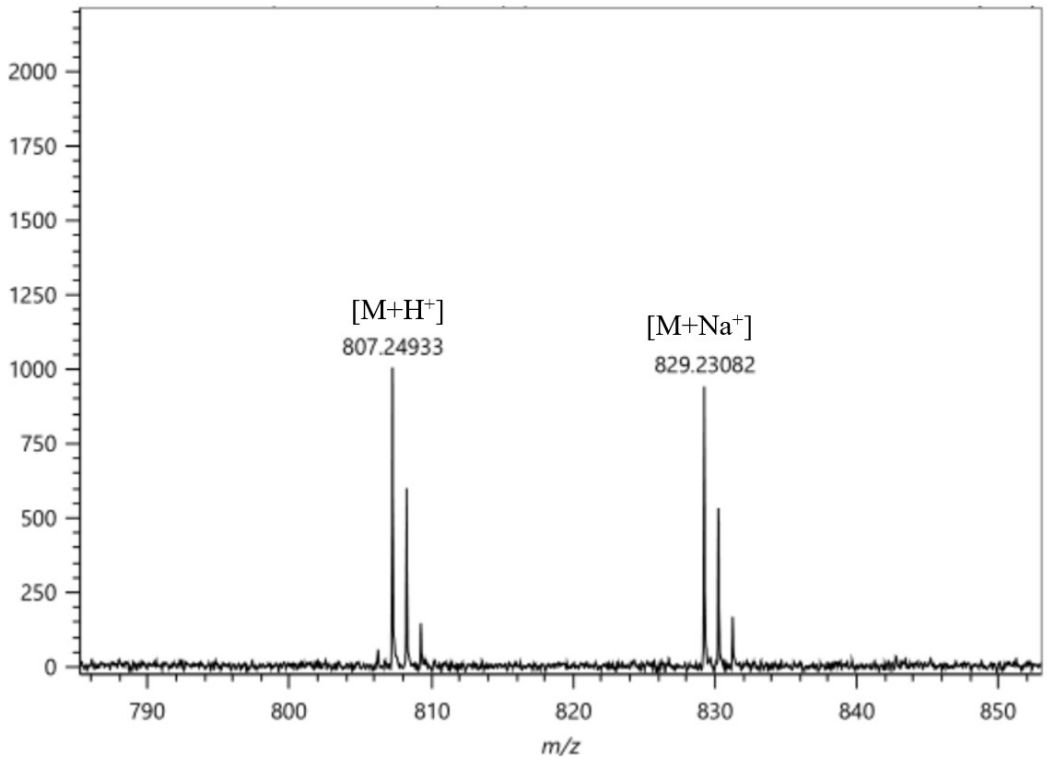

Figure S29. HRMS spectra of ***S*-3**.

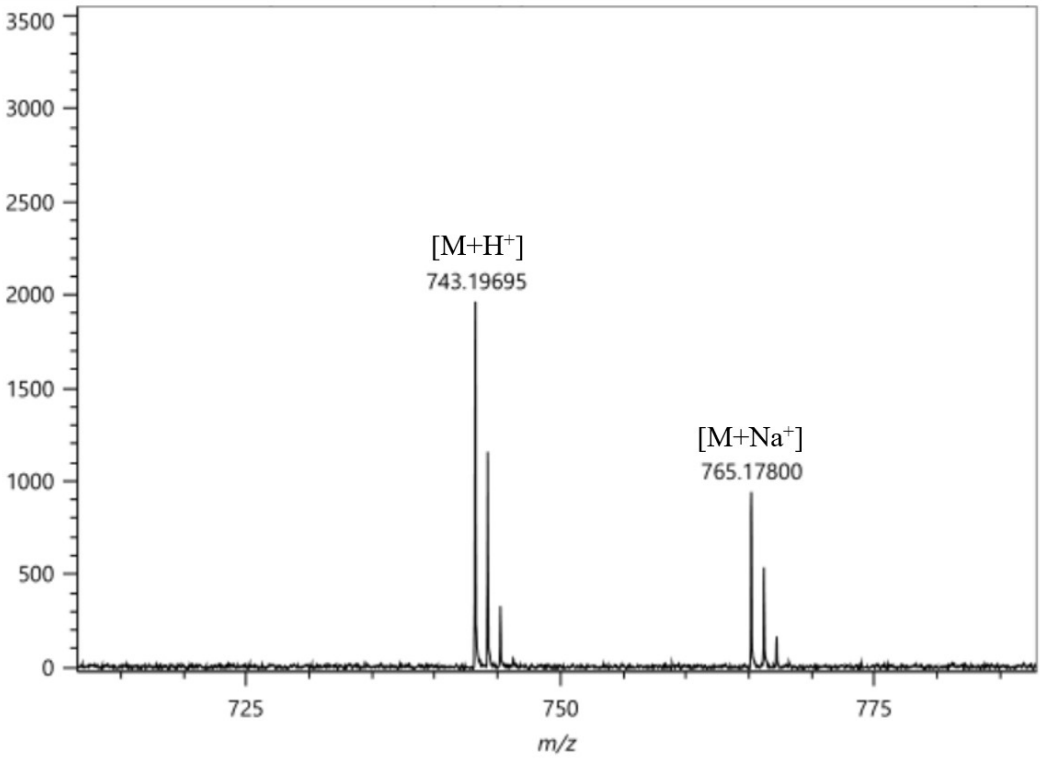

Figure S29. HRMS spectra of **(*S*,*M*)-DCzAO1**

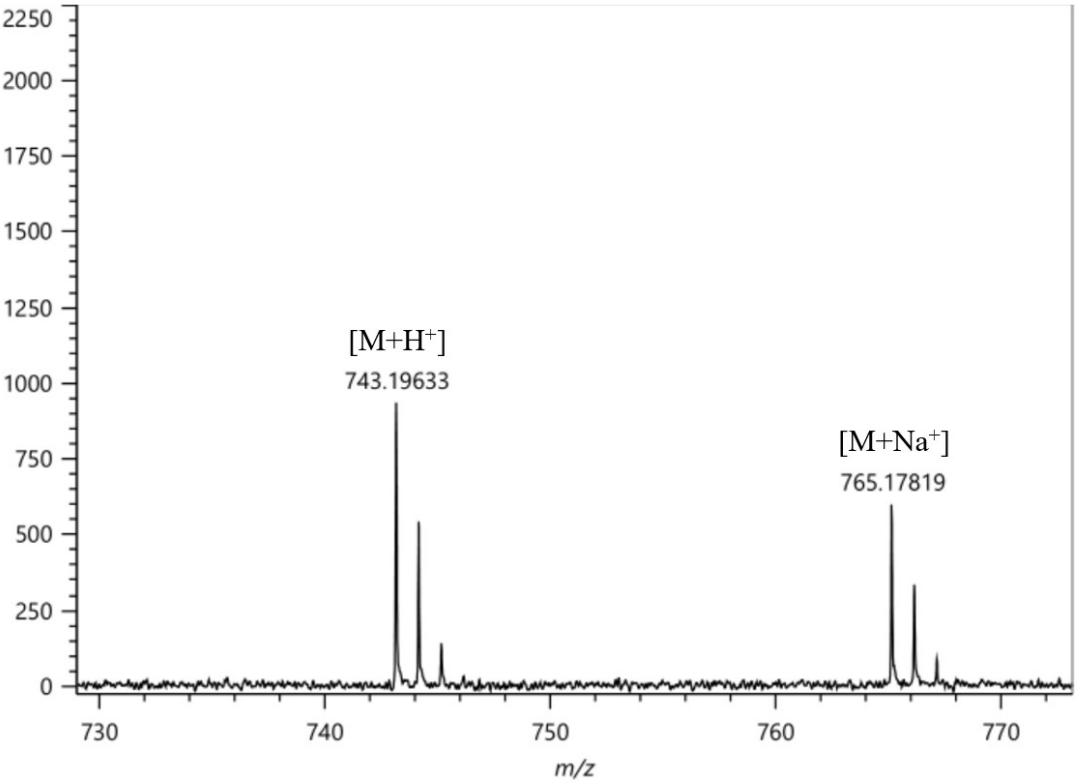

Figure S30. HRMS spectra of **(*S*,*P*)-DCZAO2.**